

Lawrence Livermore Laboratory

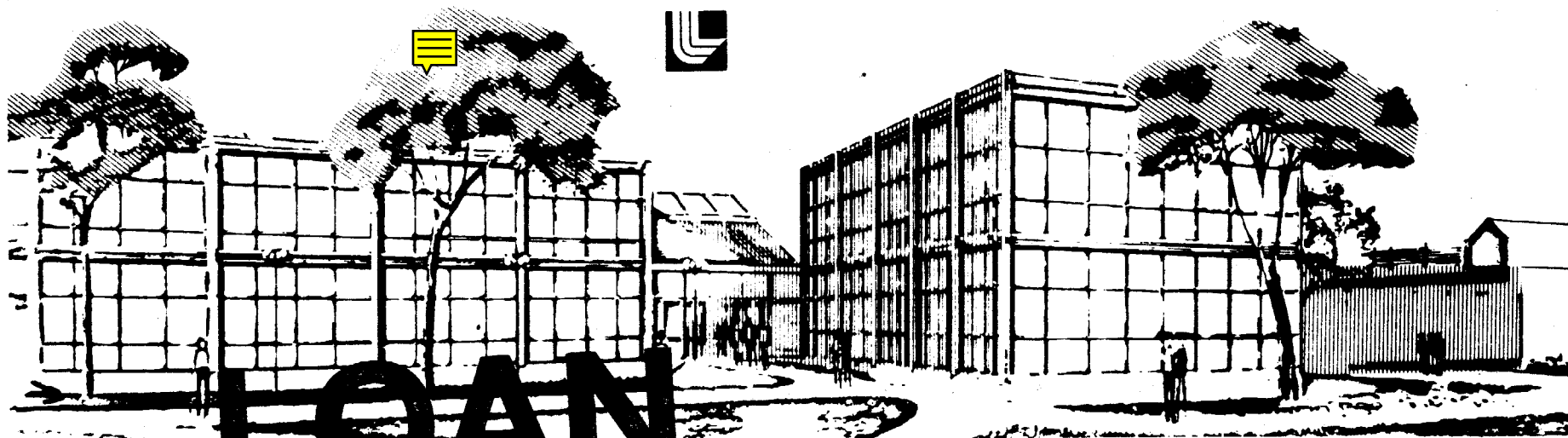
This is a preprint of a paper intended for publication in a journal or proceedings. Since changes may be made before publication, this preprint is made available with the understanding that it will not be cited or reproduced without the permission of the author.

ADPIC - A THREE-DIMENSIONAL PARTICLE-IN-CELL MODEL FOR THE DISPERSAL OF ATMOSPHERIC POLLUTANTS AND ITS COMPARISON TO REGIONAL TRACER STUDIES

Rolf Lange

August 1977

This paper was prepared for submission to
Journal of Applied Meteorology



LOAN

COPY

CIRCULATION COPY
SUBJECT TO RECALL
IN TWO WEEKS

DISCLAIMER

This document was prepared as an account of work sponsored by an agency of the United States Government. Neither the United States Government nor the University of California nor any of their employees, makes any warranty, express or implied, or assumes any legal liability or responsibility for the accuracy, completeness, or usefulness of any information, apparatus, product, or process disclosed, or represents that its use would not infringe privately owned rights. Reference herein to any specific commercial product, process, or service by trade name, trademark, manufacturer, or otherwise, does not necessarily constitute or imply its endorsement, recommendation, or favoring by the United States Government or the University of California. The views and opinions of authors expressed herein do not necessarily state or reflect those of the United States Government or the University of California, and shall not be used for advertising or product endorsement purposes.

ADPIC - A THREE-DIMENSIONAL PARTICLE-IN-CELL
MODEL FOR THE DISPERSAL OF ATMOSPHERIC POLLUTANTS
AND ITS COMPARISON TO REGIONAL TRACER STUDIES

Rolf Lange
Lawrence Livermore Laboratory, University of California
Livermore, CA 94550

August 1977

ABSTRACT

A hybrid Lagrangian-Eulerian atmospheric transport-diffusion model was developed to calculate the three-dimensional distribution of atmospheric pollutants in transient-region flow fields. This Atmospheric Diffusion Particle-in-Cell (ADPIC) code was validated against several existing closed-form analytical solutions including a puff release in steady, unidirectional shear flow, and a puff release with scale-dependent horizontal and vertical eddy diffusion coefficients. These tests showed that the ADPIC results were within a 5 percent error when compared to the analytic solutions. Regional (100 km) tracer studies at the National Reactor Test Station Idaho Falls, Idaho, and at the Savannah River Laboratory, Aiken, South Carolina, were also used to compare the code against field measurements.

I. INTRODUCTION

The Atmospheric Diffusion Particle-in-Cell (ADPIC) code is a numerical, three-dimensional, Cartesian, particle-diffusion code capable of simulating the time-dependent distribution of air pollutants under many conditions. These conditions include space and time varying wind fields, calm conditions, space-variable surface roughness, wet and dry deposition, radioactive decay, and space- and time-variable diffusion parameters.

Basically, the code solves the three-dimensional advection-diffusion equation in its flux conservative form (pseudoveLOCITY technique) for a given non-divergent advection field by finite difference approximations in Cartesian coordinates. The method is based on the particle-in-cell technique with the pollutant concentration represented by Lagrangian-marker particles inside a fixed Eulerian grid (Welch, Harlow, Shannon and Daly, 1965; Amsden, 1966; Shlarew, Fabrik and Prager, 1971; Lange, 1973). Most air pollution scenarios involve time- and space-varying advection fields (shear) and diffusion parameters. They may involve topography, deposition from various effects for a variety of active or inert source and are inherently three-dimensional in nature. ADPIC was developed to model these aspects of pollutant dispersal as a function of time for specified source terms with the exception, for the present, of photochemistry.

With the development of the three-dimensional non-divergent (mass-conservative) windfield model MATHEW (Sherman, 1977), which is used to provide the full three-dimensional space- and time-varying advection field to ADPIC, pollutant dispersion studies of considerable complexity can be undertaken.

ADPIC has undergone various validation tests against closed analytic solutions and regional tracer studies. The computed standard deviations are within 5% of those of selected analytic solutions (Lange, 1973). Agreement is remarkably consistent against methyl iodine tracer studies at NRTS, Idaho Falls, Idaho and ⁴¹Ar plumes at Savannah River Laboratory, Aiken, South Carolina. ADPIC concentrations are 60% of the time within a factor of 2 and 95% of the time within an order of magnitude of measurements without any tuning of the adjustable parameters of the model to any specific site, tracer scenario, or tracer material. As such, these yet partial validation results can be viewed as an emerging indicator of the degree of accuracy with which the ADPIC-MATHEW package can compute complex regional pollutant concentration and deposition distributions.

2. DESCRIPTION OF ADPIC

The pseudo-velocity method consists of the following: given the non-linear transport-diffusion equation

$$\frac{\partial \chi}{\partial t} + \vec{U}_A \cdot \nabla \chi = \nabla \cdot (K \nabla \chi) \quad (1)$$

where χ is a scalar concentration, K is the diffusion coefficient and \vec{U}_A the (given) non-divergent advection velocity field, we can, under the assumption of incompressibility, replace the $\vec{U}_A \cdot \nabla \chi$ term by $\nabla \cdot (\chi \vec{U}_A)$, South Carolina, were also used to compare the code against field measurements.

$$\frac{\partial \chi}{\partial t} + \nabla \cdot \left[\chi \left(\vec{U}_A - \frac{K}{\chi} \nabla \chi \right) \right] = 0 \quad (2a)$$

$$\frac{\partial \chi}{\partial t} + \nabla \cdot (\chi \vec{U}_p) = 0 \quad (2b)$$

where $\vec{U}_p \equiv \vec{U}_A - \frac{K}{\chi} \nabla \chi$ is defined as pseudo-transport velocity. The advection field \vec{U}_A is generally supplied by a non-divergent three-dimensional wind field model like MATHEW (Sherman, 1977). The term $-\frac{K}{\chi} \nabla \chi$ is a diffusivity velocity \vec{U}_D .

The grid mesh of the code is represented by an Eulerian grid consisting of three-dimensional rectangular cells of uniform size. The concentrations χ are defined at the centers of the cells and the velocities \vec{U}_A , \vec{U}_p and $\vec{U}_D = -\frac{K}{\chi} \nabla \chi$ are defined at the cell corners. The locations of the particles, which represent the pollutant cloud are defined by their individual coordinates within the fixed grid.

A time cycle of the code is divided into an Eulerian step and a Lagrangian step and proceeds as follows:

- Eulerian Step: The concentrations χ , given for each cell at the beginning of the cycle, are used to calculate the diffusivity velocities $\vec{U}_D = -\frac{K}{\chi} \nabla \chi$ which are then added to the wind advection velocities \vec{U}_A to yield a pseudo-velocity \vec{U}_p for each cell corner.
- Lagrangian Step: Each marker particle contained in a given cell is transported for one time step ΔT with a velocity \vec{U}_p , which is computed from the pseudo-velocities \vec{U}_p at the corners of the cell by a linear interpolation scheme. The new particle coordinate provide the full three-dimensional space- and time-varying advection field to ADPIC, pollutant dispersion studies of considerable complexity can be undertaken.

$$\vec{R}_{T+\Delta T} = \vec{R}_T + \vec{U}_p \cdot \Delta T \quad (3)$$

Finally, a new concentration distribution χ is calculated from the new particle positions, thus ending the cycle.

The Eulerian-Lagrangian particle-in-cell method has three desirable features of great importance. First, the fictitious Eulerian numerical diffusion is eliminated because the particles representing the pollutant concentration are transported and diffused along the Pseudo-velocity stream lines defined for each particle by $\vec{U}_p(x,t)$. Second, each marker particle can be tagged with its coordinates, age since generation, mass, activity, species and size, which greatly facilitates the parameterized computation of wet and dry deposition, radioactive decay, particle size distributions, and reaction rates of a pollutant. Third, three dimensional particle-in-cell codes are relatively fast running in part because computations are only made for those cells that contain particles. Although, there are other schemes available to combat fictitious Eulerian numerical diffusion by higher order advection schemes (Molenkamp 1968) or spectral methods, (Christensen and Prahm 1976) estimates on computer time quoted are generally based on the two-dimensional models. If extended to three dimensions on the basis of additional grid cells required, both, computer time and memory core size quickly become an additional determining factor in which numerical scheme is to be chosen.

While it is difficult to give a generally valid estimate of computational time for a complex three dimensional transport and diffusion model like ADPIC, the following description may be helpful: For a regional (100 x 100 km²) atmospheric boundary layer study with topography and three

individually different continuous pollutant sources, ADPIC uses 24 000 cells (40 x 40 in the horizontal, 15 in the vertical) and 30 000 particles (simultaneously present in grid). In this mode, ADPIC requires about 90% of large-core memory, and runs about 50 times faster than real time, on a CDC 7600 computer.

Interpolation and truncation errors inherent in the finite difference algorithms remain, of course, and must be dealt with by the choice of the time step and cell size.

ADPIC uses staggered grids in which the velocities \vec{U} and diffusivities K are defined at the cell corners while the concentrations χ are defined at cell centers. This has the following two important advantages over non-staggered grids.

The finite difference algorithm for the diffusion velocity in ADPIC, reduced to one dimension, is

$$U_{D_{i+1/2}} = - \frac{K_{i+1/2}}{\Delta X} \cdot \frac{(x_{i+1} - x_i)}{\frac{1}{2}(x_{i+1} + x_i)} \quad (4)$$

where $U_{D_{i+1/2}}$ and $K_{i+1/2}$ are the diffusion velocity and the diffusivity at the cell corners $i+1/2$, and x_{i+1} and x_i are the concentrations at the $i+1$ and i cell centers and ΔX is the cell size. For non-staggered grids this expression takes the form

$$U_{D_i} = - \frac{K_i}{2\Delta X} \frac{(x_{i+1} - x_{i-1})}{x_i} \quad (5)$$

The advantages of Eq. (4) over (5) are that the diffusion velocity U_D does not become infinite when the concentrations in the denominator go to zero,

and that only one layer of cells around the outside of the grid is required to specify the boundary conditions.

When the expression for the diffusivity velocity U_D , Eq. (4), is expanded in a Taylor series and a Gaussian concentration distribution is chosen and substituted for χ into this series expansion, one obtains an expression for the truncation error of U_D in form of a ratio of the ADPIC diffusivity velocity U_D divided by the exact differential expression for the diffusivity velocity $U_D = -K \frac{\partial \chi}{\partial x}$. In one dimension and retaining only the highest error term, this ratio is

$$\frac{U_D(\text{ADPIC})}{U_D(\text{exact})} = 1 - \left(\frac{\Delta x}{2\sigma_x} \right)^2 \quad (6)$$

where Δx is the grid cell size and σ_x is the standard deviation of the assumed Gaussian concentration distribution. Equation (6) indicates that by choosing enough cells to resolve a pollutant distribution, i.e., $\sigma_x \geq 2\Delta x$, the truncation error can be made as small as desired.

Due to the part-Eulerian, part-Lagrangian nature of ADPIC, the boundary conditions break up into one set of conditions imposed on the Eulerian velocity field and one set imposed on the Lagrangian particles. Both sets must be consistent with each other.

The two basic boundary conditions imposed on the pseudo-velocity field in ADPIC $\vec{U}_p = \vec{U}_A + \vec{U}_D$ are constant mass flux, $(\chi \vec{U}_p) = \text{constant}$, corresponding to inflow and outflow of particles, and zero mass flux $(\chi \vec{U}_p) = 0$, corresponding to reflection of particles from the boundary. There are intermediate cases as, for example, deposition of particles on the topography, in which case a deposition velocity is specified. In the kind of studies

that ADPIC has so far been used for, the concentration field is smooth enough by the time it reaches the outflow boundary that the outflow boundary condition can be specified by postulating a constant flux of particles through the boundary grid cell layer.

The particle boundary conditions are very simple. If a particle has been found to have left the grid during a cycle, it is either annihilated or counted as deposited or is reflected, according to the type of boundary specified.

3. VERIFICATION OF ADPIC AGAINST ANALYTICAL SOLUTIONS

Selected analytic solutions to the diffusion-advection Eq. (1) were chosen in order to verify the ADPIC code. Because of the intractability of this equation analytic solutions exist for only rather simple, linearized cases with Gaussian pollutant distributions. Table 1 summarizes the cases chosen for the basic verification of ADPIC. Overall, ADPIC results agreed with the closed Gaussian solutions to within a 5% error (Lange 1973). The time and spacial scales and other parameters, like source configuration and diffusion parameters, were chosen in such a way as to make the verification cases compatible with scale relations in the real atmosphere. On this basis the 5% maximum error between ADPIC and analytic solutions holds over regional scales of many hours and hundreds of kilometres. There is no indication that this error will increase if the cases described in Table 1 were run for even much longer periods or larger distances.

An example, puff-diffusion in simple vertical shear flow (case 3 of Table 1), is discussed in the following. The analytical solution

for comparison has been worked out (Quesada and MacLeod 1971). A version of ADPIC is used in which the Eulerian grid mesh automatically expands with the growth of the puff.

A 20 x 20 x 20 cell three dimensional grid mesh is constructed so that the initially spherically symmetrical puff with Gaussian distribution is generated by a random number generator. Figure 1 displays the distribution of Lagrangian marker cells at approximately 5 s in the x, z plane in unbounded shear flow. A strong shear $\frac{\partial U}{\partial z} = 0.125 \text{ s}^{-1}$ was chosen.

Figure 2a compares the analytical solution with the ADPIC solution of the number of particles per cell as a function of distance in the x, z plane at approximately 6300 s. Figure 2b shows the distribution of the pollutant after deformation transport and diffusion in the unbounded shear flow. Figure 3 shows relative cloud-center concentration as a function of time for the shear flow case.

While these simple test cases in no way represent a full verification of the model, the results indicate that on the basis of the gradient theory of turbulence the ADPIC code represents a reasonably accurate calculational framework for attacking transport-diffusion problems for simple flow fields in multi-dimensional space. If a flow field in the real atmosphere by suitable Reynold's averaging is separated into a mean wind field \vec{U}_A and a turbulent diffusive component \vec{U}_D , and is identified as the pseudo-velocity field $\vec{U}_P = \vec{U}_A + \vec{U}_D$ (Eqns. 2 and 3), then the quality of the ADPIC solutions for the real atmosphere, is governed by our knowledge of the temporal-spatial regional flow fields and the spatial distribution and time dependency of the eddy-diffusion processes, and source terms.

4. VALIDATION OF ADPIC AGAINST A REGIONAL TRACER STUDY AT THE IDAHO FALLS NRTS SITE

For the past several years, the National Oceanic and Atmospheric Administration has performed regional tracer tests at the Idaho Falls National Reactor Test Station (NRTS). The NRTS staff provided both the meteorological and source-term information for one of their methyl iodine releases. That test consisted of a 3-h injection of methyl iodine with ^{131}I into a transient regional flow field. Meteorological properties were documented by 17 meteorological towers as well as by upper level wind measurements and indicated a Pasquill C category. Thirty-six volume samplers were arranged in the field in four arcs at various distances downwind from the source.

The regional flow field was calculated by the LLL three dimensional mass-conserving wind field code MATHEW (Sherman 1977). ADPIC simulated the time history of the passage of the cloud over each of the samplers while also calculating the total spatial-temporal distribution of the pollutant. The details of the ADPIC problem setup and a summary of the results are included in Table 2. The horizontal eddy diffusion coefficient K_h in m^2/s was obtained directly from the Pasquill Category C standard deviation σ_y in m through the relationship (Slade 1968a and Walton 1972)

$$K_h(t) = \frac{1}{2} \frac{d(\sigma_y^2(t))}{dt} = \bar{U} \sigma_y \frac{d\sigma_y}{dx} \quad (7a)$$

with

$$\sigma_y = .17 x^{.92} \quad (7b)$$

where \bar{U} is the local mean wind in m/s and x the distance along the plume axis in m. The vertical eddy diffusion coefficient used was

$$K_z = \begin{cases} .1z & \text{for } 0 \leq z \leq 100 \text{ m} \\ 10 & \text{for } z > 100 \text{ m} \end{cases} \quad (8)$$

As an aid to interpreting the results, Fig. 4 shows an illustration of the complex topography of the Idaho Falls region and the general outline of the plume as it was transported downwind from its source. (The vertical scale is approx. 50 times horizontal scale).

Fig. 5 shows the projection of the Lagrangian marker particles representing the cloud onto the horizontal plane and the sampler arcs at 3 h. The jagged left edge of the pollutant cloud is caused by topographical and grid resolution effects.

ADPIC samples concentration by counting those Lagrangian particles that pass through a sampler volume. Such a simulated ADPIC surface-air concentration history at sampler A-3 is shown in Fig. 6 and is compared in terms of its breadth with the actual passage time of the plume as documented by field measurements. Unfortunately the field measurements gave only total time integrated concentrations and time of passage. Therefore comparison with ADPIC was only possible on the basis of the total area under the ADPIC sampler curves like the one in Fig. 6.

Figure 7 shows the time integrated concentration of the samplers along arc C as a function of crosswind distance for both ADPIC and field measurements. These integrated concentrations are also compared with the results obtained by solutions using a Gaussian plume equation for the stability category C. The Gaussian plume result in Fig. 7 was overlaid on what was considered to be the main branch of the ^{131}I plume and was not based on the

wind speed and direction at the source. If the Gaussian plume had been based on the wind at the source, it would have partially missed the sampler arc C in Fig. 7. Although the Gaussian solution matches the peak concentration at what might be construed as the plume centerline, it is too narrow and the second peak cannot be accounted for. The second peak is a result of temporal changes in the regional flow field and an effect of the topography.

Figure 8 is a scatter diagram comparing the ADPIC time integrated ^{131}I surface air concentrations with measured values for all 36 samplers. The sources of error result from the prescription of the regional flow field, the prescription of eddy diffusion coefficients as derived from bulk meteorological parameters, and the sensitivity of the surface-air concentration to the representation of topography in the MATHEW and ADPIC codes.

5. COMPARISON OF ADPIC AGAINST THREE ^{41}Ar PLUMES AT SAVANNAH RIVER LABORATORY, SOUTH CAROLINA

During Spring 1974, three daily 6-h exercises were initiated to compare ADPIC against data from three ^{41}Ar plumes at the Du Pont Savannah River Plant (SRP) in Aiken, South Carolina. Because of their typical difference in synoptic condition, the second and third test scenarios were chosen as detailed validation experiments for ADPIC. Test 2 had mostly light 1 to 3 m/s winds varying over more than 180° during the 6-h test while Test 3 had rather steady 1 to 4 m/s winds varying over less than 90° during the

test. Both tests started at 8:00 a.m. Eastern Daylight Time with approximately an F-Pasquill stability and a temperature inversion at a height of about 140 m breaking up an hour or so later. Both tests ended at 2:00 p.m. EDT with approximately a C-Pasquill stability.

Figure 9 shows the SRP site with the C, K, and P reactors, which are the sources for the three ^{41}Ar plumes, each having a stack height of 60 m. The topography of the site and its surroundings varies over about 75 m, mostly because of the Savannah River bed; it is alternately open grass land, crops, and young pine forest. In the models topography protrudes in rectangular building block fashion into the grid from below.

The meteorological data for wind speed, direction, and their turbulent intensities (sigmas), were taken at 5-s intervals at a height of 60 m from two site towers in the P and H area, and at several heights up to 360 m from the WJBF-TV tower located 30 km northwest from the site center. In addition to providing the vertical variation of the windfield, the TV tower also provided the vertical temperature profile.

The measurements of ^{41}Ar concentrations from the three reactor plumes were obtained by looking at the peak- γ window of the radioactive ^{41}Ar with sodium iodide crystals. For Test 2, measurements were taken by two detector-equipped cars at a 2-m height at 20 different 10-min sampling stops. To track the plumes the sampling stops were made anywhere within about a 25 km radius from the sources as permitted by the road network. For Test 3, in addition to 22 measurements from the two cars, a detector-equipped helicopter from EG&G, Inc., Las Vegas, Nevada, tracked the plumes at heights of 150 and 300 m above topography. The helicopter flew a total of 19 more or less straight-line sampling passes (at speeds of about 50 m/s) each of which lasted approximately 3 to 7 min and collected data at 6-s intervals.

The ADPIC validation problem setup for the Savannah River plumes and comparison of results with measured data is shown in Table 3. The three-dimensional mass-consistent advection field \vec{U}_A was provided by the MATHEW (Sherman, 1977) code in 15-min-averaged data sets using interpolated data from the three meteorological towers. The three plume sources were modeled by continuous generation of ADPIC particles, each representing a fixed amount of activity and possessing an "age" label to allow for radioactive decay calculation according to the ^{41}Ar decay constant of $1.04 \times 10^{-4} \text{ s}^{-1}$. Typically, at any given time about 12 000 particles were present in the grid to represent the plumes.

The horizontal diffusion coefficients K_H were obtained directly from the rms wind direction fluctuations σ_θ as measured on the TV-tower at heights of 10, 36, 91, 137, 243 and 335 m. The relationships used are (Walton 1972, Tennekes 1972a and Slade 1968b)

$$K_H = \frac{1}{2} \frac{d}{dt} (\sigma_y^2) \quad \text{with} \quad \sigma_y = \sigma_\theta |\vec{r}|^{0.91}, \quad (9a)$$

where σ_y is the standard deviation of the plume width, $|\vec{r}|$ is the distance from the source along the plume axis, and d/dt is the time derivative. If $|\vec{r}|$ is replaced by $\bar{U} \cdot t$ assuming Taylor's hypothesis (Tennekes 1972a) where U is the local mean wind speed in m/s and t is the time in s since a pollutant parcel has left the source, Eqn. 9 becomes

$$K_H = \sigma_y \frac{d\sigma_y}{dt} \quad \text{with} \quad \sigma_y = \sigma_\theta (\bar{U} \cdot t)^{0.91} \quad (9b)$$

Since ADPIC models a continuous source by a time sequence of instantaneous puffs released one per time step, and since σ_θ is measured as a function of height, U is known from the wind field, and t is the age of the puff since

generation at the source, Eqn. 9b permits the computation of K_H for each puff as a function of position and time.

Because reliable vertical wind fluctuation data were not available, the vertical diffusion coefficients K_z were given the following form

$$K_z = \begin{cases} \frac{(K_z)_H}{H} z & , \quad 0 \leq z \leq H \\ (K_z)_H & , \quad H < z \end{cases} \quad (10)$$

where $(K_z)_H$ is K_z at some height H , generally the top of the constant flux layer, and z is the height above the surface. Typical values for $(K_z)_H$ for the stable to unstable conditions encountered were picked from SRP data (Crawford, 1974) which are based on the time-lag with height analysis of temperature maxima and minima (Sutton 1953), and varied from 1 to 25 m^2/s . H varied from 10 to 100 m. Elevated inversions were modeled in ADPIC by setting $K_z = 0$ at and above the inversion height.

Sampling is done in ADPIC by counting particles, each representing a certain amount of activity. For comparison with field data, ADPIC simulated the sampling at the fixed car locations and also simulated a moving detector to model five of the helicopter flights. Figure 10 shows the ADPIC particle simulation of the C, P, and K plumes together with one of the helicopter runs. Figure 11 is a typical example of data obtained by real and ADPIC helicopters.

Figure 12 shows the results of the ADPIC comparison with measurements for cars (Test 2 and Test 3) and also for helicopters (Test 3). Shown are the relative air concentrations for 40 surface samplers and 9 helicopter flights. As already indicated in Table 3, about 60% of the time the ^{41}Ar plume concentrations computed were within a factor of 2 of measured, while 98% of

the time they agreed within an order of magnitude. In more detail, ADPIC agreed better with the car data of Test 3 than of Test 2. This is a result of the major difference between the two tests in the most sensitive parameter, namely the variability of wind direction which was high during Test 2 in contrast to the much steadier Test 3 conditions. The enormous sensitivity of the regional air concentrations to wind direction for the case of point sources is illustrated by Figs. 13 through 16.

Figures 13 and 14 show the ADPIC plumes for the C, P, and K reactors for Test 2 at 12:00 and 13:00 EDT. In one hour, the winds have swung from easterly to southerly to westerly, resulting in the breakup of the plumes of Fig. 13. This shift literally paints a 180° sector before new steadier winds begin to establish new plumes as shown in Fig. 14. Figures 15 and 16 represent the corresponding ADPIC isopleths at a height of 2 m together with the detector car locations at those times. The choppiness of the contours is caused by topography and grid resolution. Keeping in mind the scale of the figures an appreciation can be gained for the difficulty of plume air concentration data collection (plume chasing) on the regional scale. In addition to the gross effects of the wind direction variability discussed, Figures 13 through 16 also show the local difference in the advection field as depicted by the difference in direction of the three simultaneous plumes.

On the regional scale, data collected by one moving detector (moving fast compared with wind speeds, such as the helicopter used in Test 3) are more conclusive than even a large number of fixed surface detectors at least for variable winds. Figure 11, showing concentration versus time for a single helicopter pass, illustrates the point: one pass of the helicopter

sampler yields a snapshot of the plume cross sections showing centerline location, maximum concentration and plume width.

Comparison of the field helicopter trace with the ADPIC model helicopter allows separation of model errors caused by the advection field (offset peaks) from errors caused by diffusion parameters (plume width and peak concentrations). Figure 11 shows that the advection field used in ADPIC was in error for the K plume while it was correct for the P plume. The reason is that the mass-consistent advection field had meteorological input data at the P reactor while it had to rely on an interpolated value at the K reactor. In addition, the diffusion parameters used in ADPIC appear to diffuse the plume somewhat too slowly.

Figure 12 shows that 89% of the time (8 out of 9 peaks) the ADPIC helicopter results were within a factor of 4 of the measured EG&G helicopter data. This is in better agreement than for the cars for the same Test 3 because peak concentrations were compared for the helicopters, thus bypassing the errors caused by advection. The reason for the very low results of ADPIC for the 9th helicopter run is that one of the EG&G helicopter passes was nearly parallel to the K plume. Because the direction of the modeled K plume was off by a few degrees the ADPIC model helicopter missed it, thus reintroducing the importance of advection errors for passes at small angles to the plume axis.

6. CONCLUSIONS

ADPIC was developed to study the pollutant dispersal and deposition on the regional (100 km) scale from a variety of sources and for given wind fields. Of special interest are those cases for which source and terrain conditions are complex and the behavior of the atmosphere is nonuniform and nonsteady. For such cases the advection field can be provided in mass-conservative form from interpolated meteorological data by a mass-consistent windfield code such as MATHEW (Sherman 1977). ADPIC computes the time-varying three dimensional concentration field of inert as well as radioactive pollutants and can treat topography, dry deposition, and inversion layers. The chief advantages of the particle-in-cell method are the lack of numerical diffusion errors present in other methods, the capability to label the Lagrangian particles with various properties like mass, activity, size, time, etc., and reasonable computer time requirements.

The code was validated against a number of closed Gaussian solutions to the diffusion-advection equation including simple wind shear and scale-dependent diffusion, and was found to be accurate to within 5% of such solutions.

Regional tracer studies using ^{131}I at Idaho Falls and ^{41}Ar plumes at Savannah River Laboratory were used to validate ADPIC against regional field data using fixed high-volume samplers, γ -detector-equipped cars, and helicopters. Without *tuning* the model parameters to any given regional site, type of source, or sampling method there appeared to emerge a uniformity in the accuracy in which ADPIC could model regional scenarios of pollutant dis-

persal as indicated by Figs. 8 and 12. Typically, 60% of the time ADPIC was within a factor of 2 of field data while 96% of the time it agreed to within an order of magnitude.

Without a doubt, it would be desirable to conduct a comprehensive parameter sensitivity study with ADPIC in order to put the results given in Figs. 8 and 12 into perspective. Unfortunately, such a task for a three dimensional time dependent code requires enormous amounts of computer time, and may have to wait for the next generation of computers.

Nevertheless, from runs for different atmospheric stabilities, varying topographical complexities, and comparison with experimental results such as those in Figs. 7, 10, 11, 15 and 16 a qualitative statement about the types of errors most important in ADPIC can be made with some confidence: For modeling plumes in the atmospheric boundary layer on the regional (100 km) scale the chief sources of error in the ADPIC model results appear to be, in decreasing order of magnitude, wind direction, topography, diffusion parameters, source strength, and wind speed.

ACKNOWLEDGMENTS

I would like to thank Leonard Lawson for programming ADPIC and for organizing efficiently the enormously large data files necessary to run ADPIC with regional three-dimensional windfields.

This work was performed under the auspices of the U. S. Energy Research & Development Administration, under contract No. 7405-Eng-48, and supported in part by the National Science Foundation.

NOTICE

"This report was prepared as an account of work sponsored by the United States Government. Neither the United States nor the United States Energy Research & Development Administration, nor any of their employees, nor any of their contractors, subcontractors, or their employees, makes any warranty, express or implied, or assumes any legal liability or responsibility for the accuracy, completeness or usefulness of any information, apparatus, product or process disclosed, or represents that its use would not infringe privately-owned rights."

"Reference to a company or product name does not imply approval or recommendation of the product by the University of California or the U.S. Energy Research & Development Administration to the exclusion of others that may be suitable."

REFERENCES*

Amsden, A. A., 1966: The particle-in-cell method for the calculation of the dynamics of compressible fluids. Los Alamos Scientific Laboratory, Report LA-3466.

Christensen, O., L. P. Prahm, 1976: A pseudo-spectral model for dispersion of atmospheric pollutants. *J. Appl. Meteor.*, 15, 1284-1294.

Crawford, T. V., 1974: Progress report dose-to-man program FY-1973. E. I. du Pont de Nemours and Co., Savannah River Laboratory, Aiken, S. C. 29801.

Lange, R., 1973: A three-dimensional computer code for the study of pollutant dispersal and deposition under complex conditions. Lawrence Livermore Laboratory Report UCRL-51462.

Molenkamp, C. R., 1968: Accuracy of finite-difference methods applied to the advection equation. *J. Appl. Meteor.*, 7, 160-167.

Quesada, A. F., and M. A. MacLeod, 1971: The determination of diffusion coefficients in a shearing flow by chemical tracer techniques. *Proc. Symp. Air Pollution, Turbulence and Diffusion*, New Mexico, 384-391.

Sherman, C. A., 1977: A mass consistent model for wind fields over complex terrain. *Journal of Applied Meteorology*, 34, xxx.

Sklarew, R. C., A. J. Fabrik, and J. E. Prager, 1971: A particle-in-cell method for numerical solution of the atmospheric diffusion equation, and application to air pollution problems. Systems, Science and Software, La Jolla, CA, Report 3SR-844.

Slade, D. H., 1968a: *Meteorology and Atomic Energy*. Energy Research and Development Administration, Report TID-24190, pp. 100-103.

Slade, D. H., 1968b: *ibid*, pp. 151-153.

Sutton, O. G., 1953: *Micrometeorology*. McGraw Hill, N.Y.

Tennekes, H., J. L. Lumley, 1972a: *A First Course in Turbulence*. MIT Press, p. 229.

Tennekes, H., 1972b: *ibid*, p. 253.

Walton, J. J., 1972: Scale dependent diffusion. *J. Appl. Meteor.*, 12, pp. 547-549.

Welch, J. E., F. H. Harlow, J. P. Shannon, and B. J. Daly, 1965: The MAC method. Los Alamos Scientific Laboratory Report LA-3425.

*Reports published as a result of research sponsored by the U.S. government are available in printed copy or microfiche from the

National Technical Information Service
5285 Port Royal Rd.
Springfield, VA 22161

TABLE 1. ADPIC verification against closed Gaussian solutions.

Case	Description
1	Instantaneous source, constant-K diffusion
2	Instantaneous source, scale-dependent K(t) diffusion
3	Instantaneous source, constant-K diffusion in simple vertical speed shear $U = U(z)$, $V = W = 0$
4	Continuous source, constant-K diffusion (calm condition)
5	Continuous source, constant-K diffusion, advection $U = 2$ m/s
6	Continuous source, constant-K diffusion, advection $U = 10$ m/s

TABLE 2. Description of ADPIC simulation of field tracer study at NRTS, Idaho Falls.

Problem setup:

Number of grid cells: $16 \times 24 \times 24 = 9216$

Vertical cell size = 50 m

Horizontal cell size = 4300 m

Stability category: Pasquill C. Details of diffusion parameters discussed in Section 4.

Source release rate = 0.379 mCi/s for 3 h. At 0.25 mCi/particles, this corresponds to 14,720 particles total.

Deposition velocity = 0.1 cm/s

Comparison between ADPIC and field-sampler results:

Agreement within factor of:	2	5	10
Fraction of total samples $\left(\frac{\text{ADPIC samplers}}{\text{Field samplers}} \right)$	0.44	0.81	0.94

TABLE 3. Description of ADPIC simulation of three ^{41}Ar plumes at SRP, South Carolina.

Problem setup:

Number of grid cells: $40 \times 40 \times 14 = 22400$

Vertical cell size: 25 m

Horizontal cell size: day 2, 500 m; day 3, 1000 m

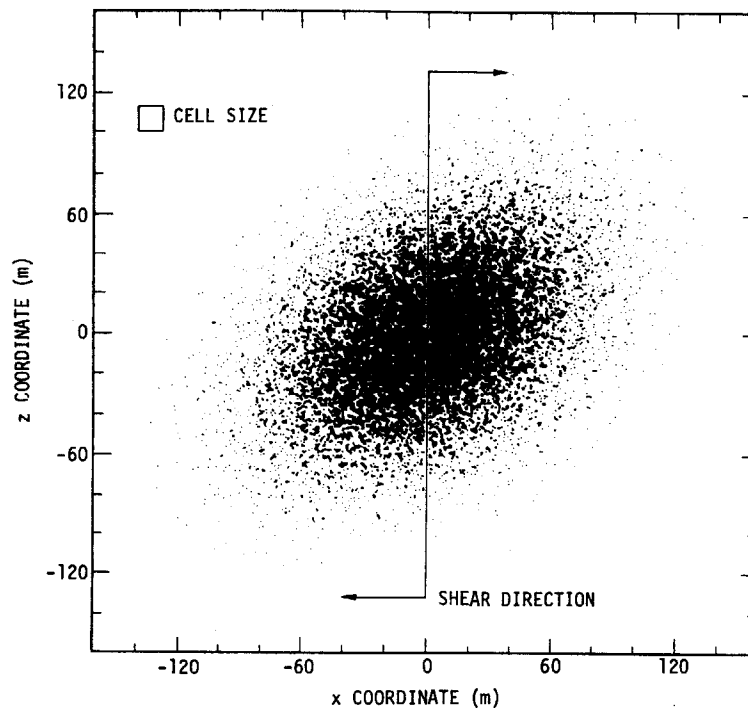
Atmospheric stability: Pasquill F through B. Details of diffusion parameters are discussed in Section 5.

Source particles: 3 continuous sources with total release rate of 3 particles per second, corresponding to approximately 65,000 ADPIC particles over a six hour release period.

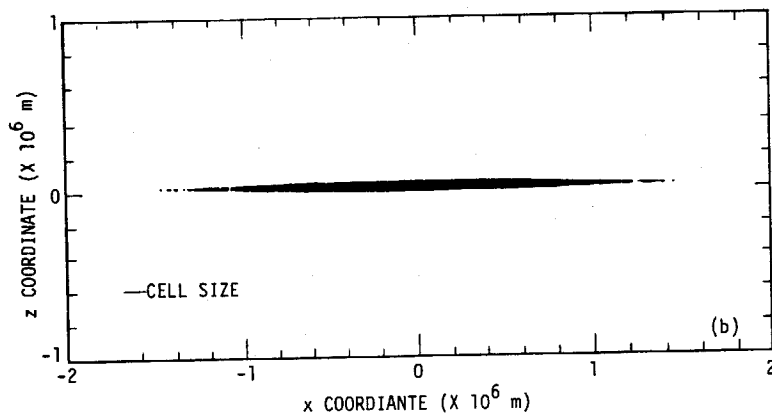
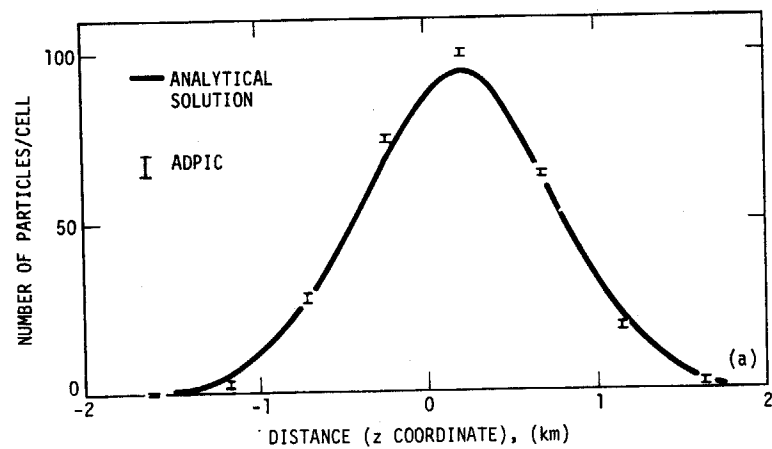
Comparison between ADPIC and measured results for both experiments:

Agreement within factor of:	2	5	10
Fraction of total samplers $\left(\frac{\text{ADPIC samplers}}{\text{Field samplers}} \right)$	0.61	0.92	0.98

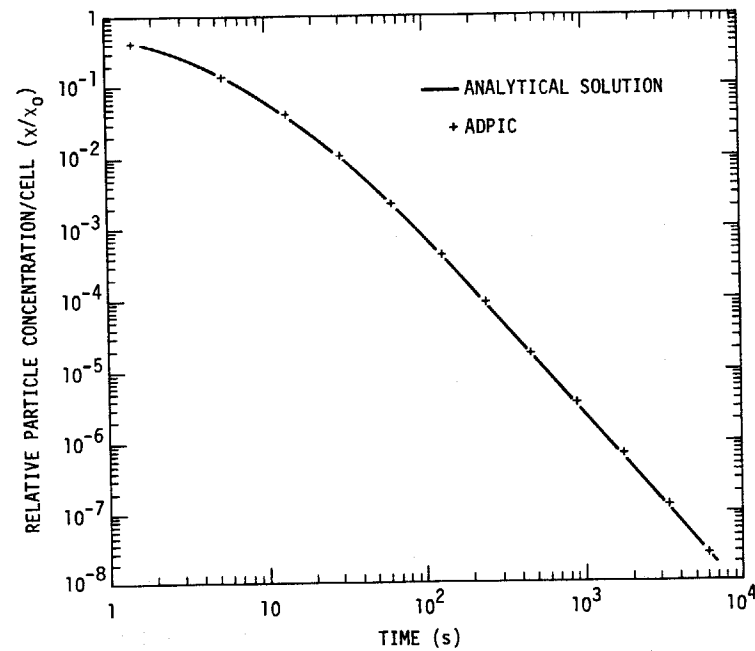
- Figure 1. Diffusion in shear flow: particle distribution at cycle 20, at $T = 5.3$ s, and in the x, z plane.
- Figure 2. Diffusion in shear flow: particle distribution at cycle 120, at $T = 6328$ s, and in the x, z plane. (a) Comparison of the analytical solution with the ADPIC solution, and (b) distribution of the pollutant after deformation transport and diffusion in the unbounded shear flow.
- Figure 3. Diffusion in shear flow: relative cloud center concentration vs time.
- Figure 4. Idaho Falls topography and plume outline.
- Figure 5. ADPIC particles representing the Idaho Falls plume after 3 h. (End of release time). Circles represent sampler locations.
- Figure 6. Activity vs. time for simulated ADPIC sampler A-3. Idaho Falls.
- Figure 7. Time integrated activity for samplers on arc C. Idaho Falls.
- Figure 8. Measured and computed time integrated ^{131}I surface air concentrations for 36 samplers at Idaho Falls.
- Figure 9. The Savannah River Plant site (SRP).
- Figure 10. Simulated helicopter flight path #838 and C, P, and K plumes as represented by ADPIC particles.
- Figure 11. Helicopter flight #838, ADPIC and measured concentrations vs. time.
- Figure 12. Measured and computed relative concentrations for three ^{41}Ar plumes at 49 samplers at SRP.
- Figure 13. C, K, and P plumes for Test 2 at 12:00 EDT as modeled by ADPIC.
- Figure 14. C, K, and P plumes for Test 2 at 13:00 EDT as modeled by ADPIC.
- Figure 15. C, K, and P plume activity isopleths from ADPIC for Test 2, 12:00 EDT.
- Figure 16. C, K, and P plume activity isopleths from ADPIC for Test 2, 13:00 EDT.



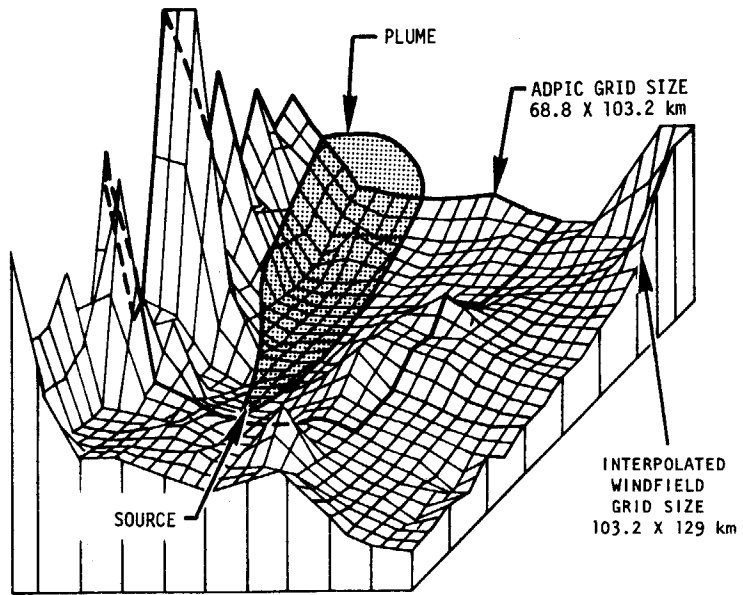
Lange - Fig. 1



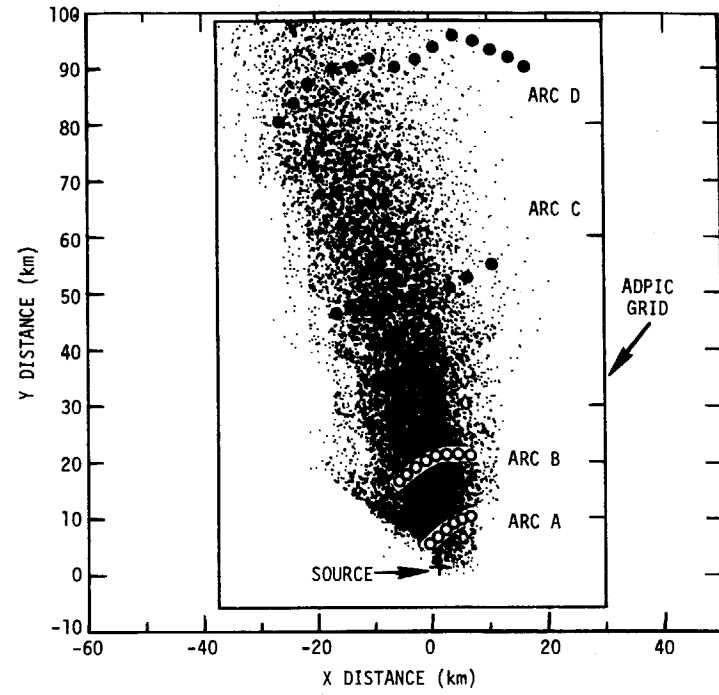
Lange - Fig. 2



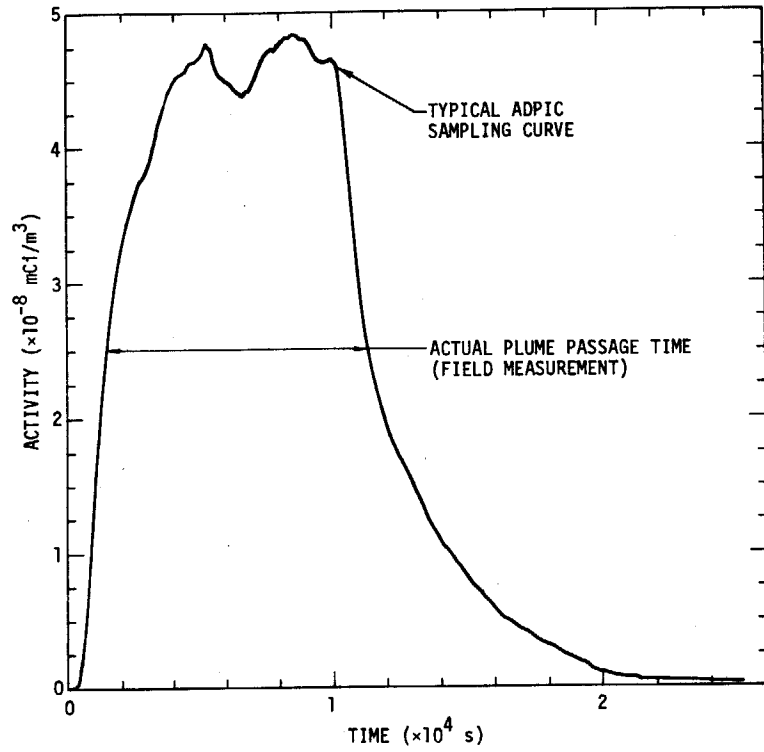
Lange - Fig. 3



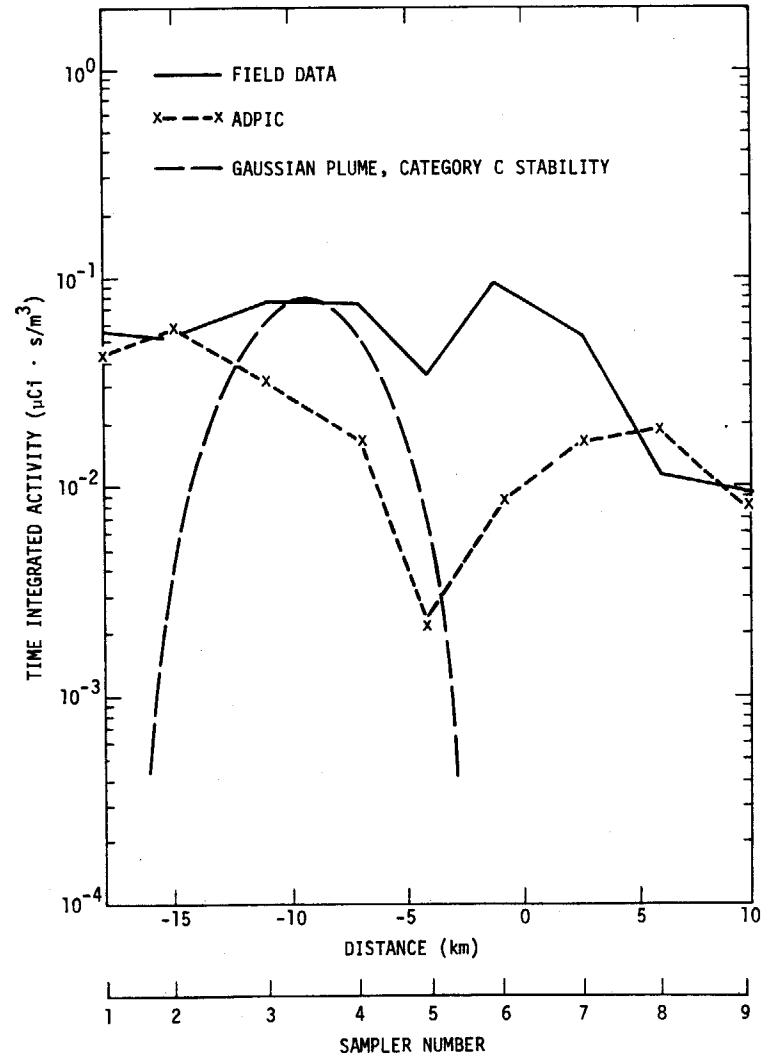
Lange - Fig. 4



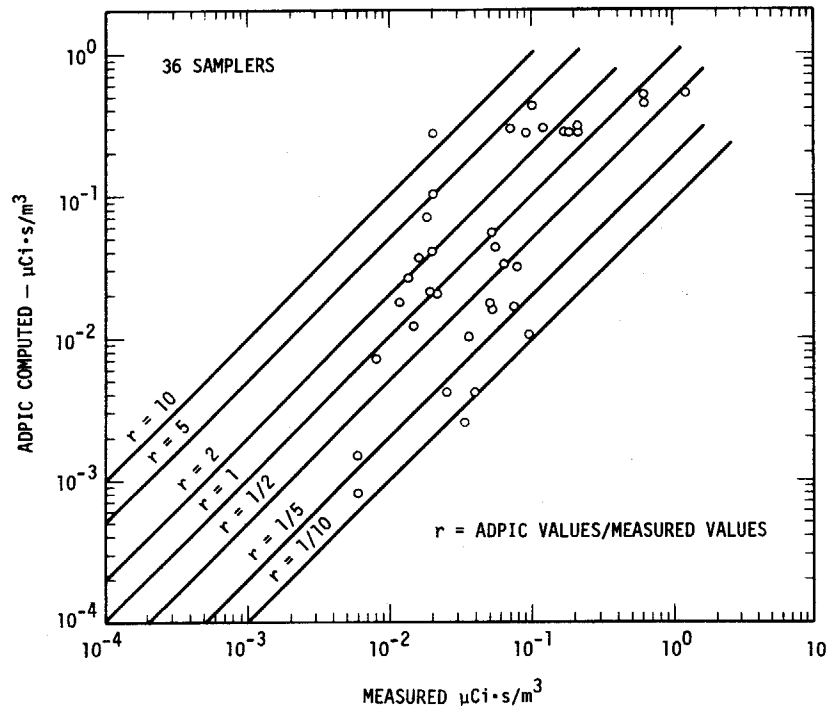
Lange - Fig. 5



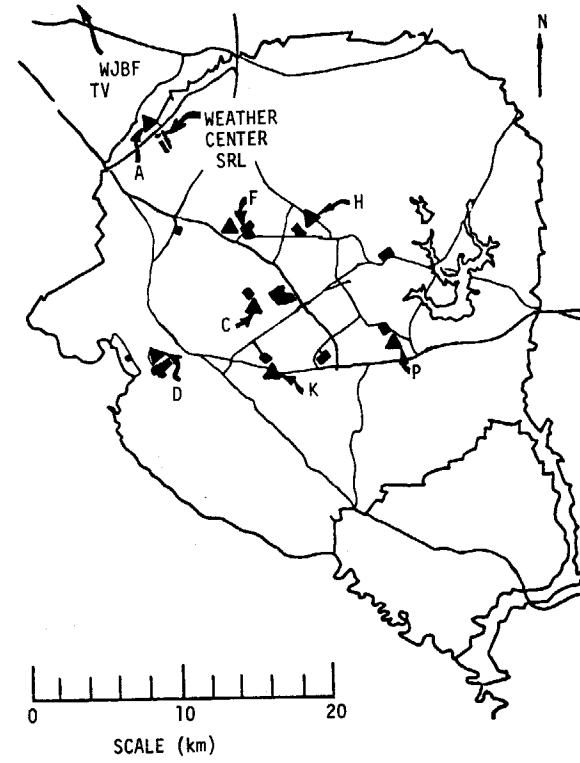
Lange - Fig. 6



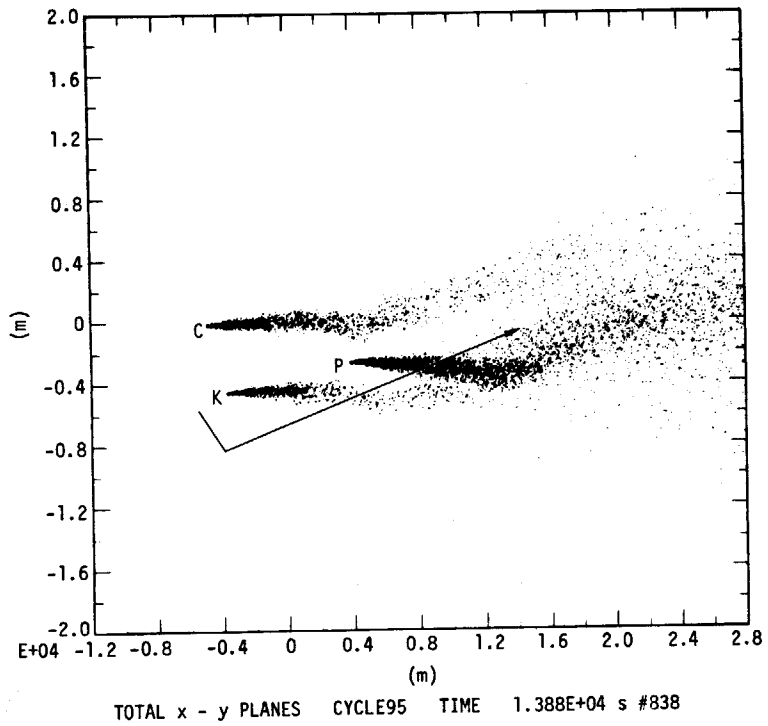
Lange - Fig. 7



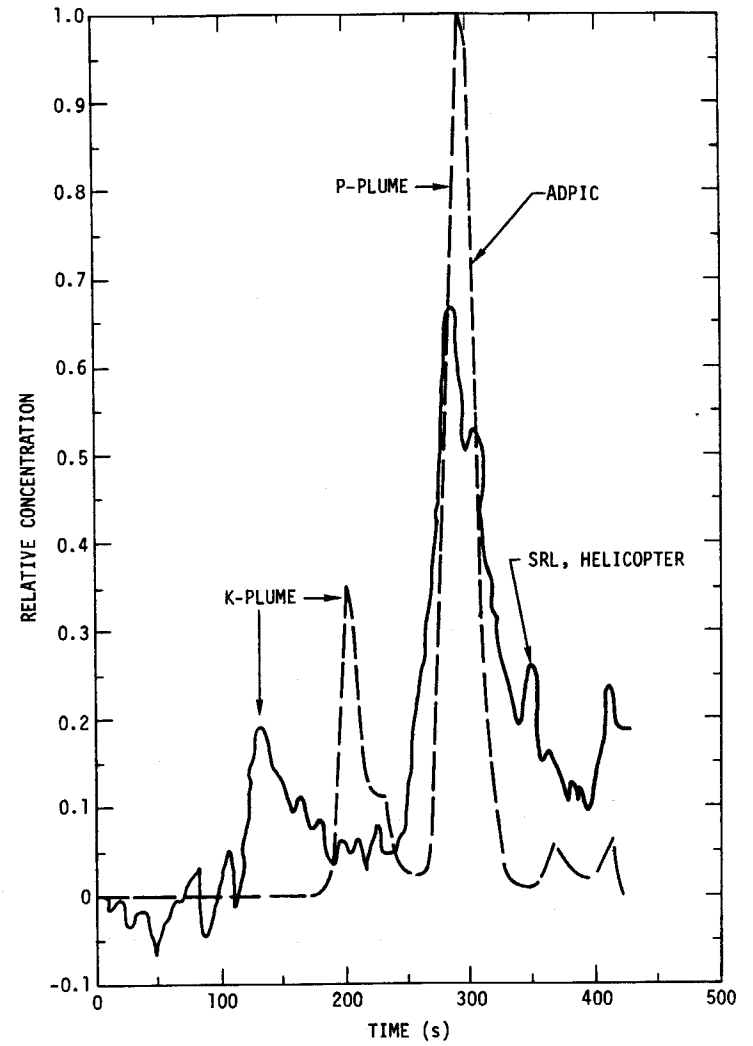
Lange - Fig. 8



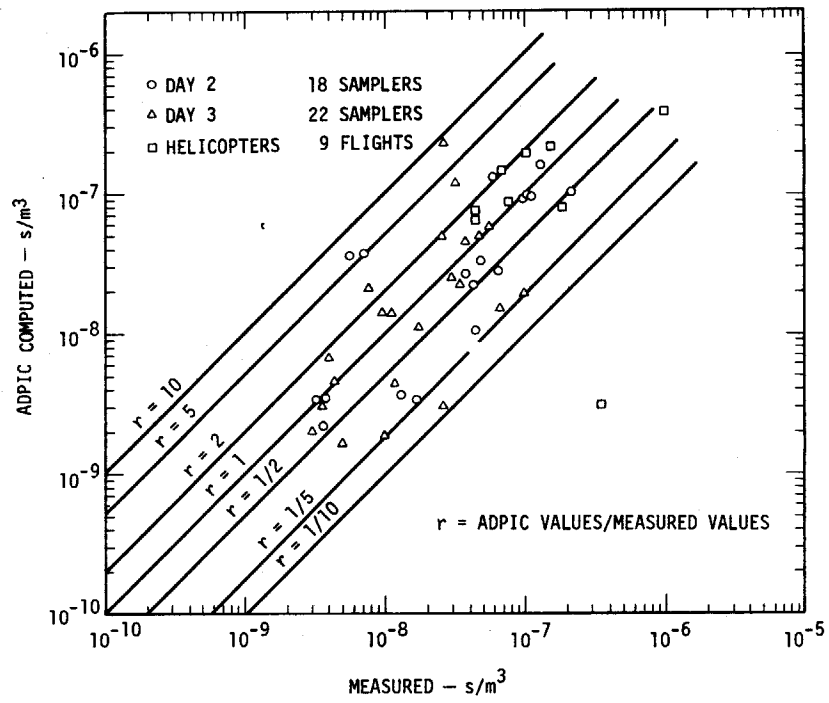
Lange - Fig. 9



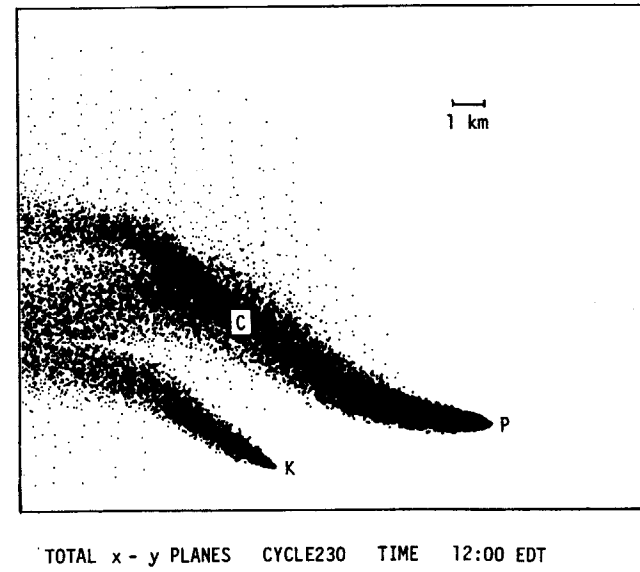
Lange - Fig. 10.



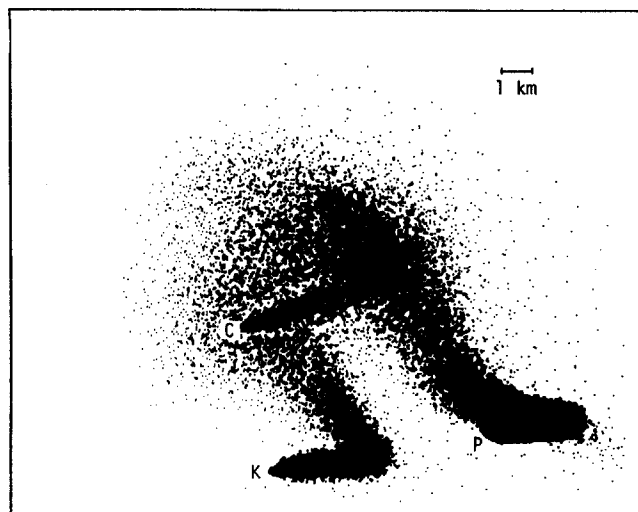
Lange - Fig. 18



Lange - Fig.12

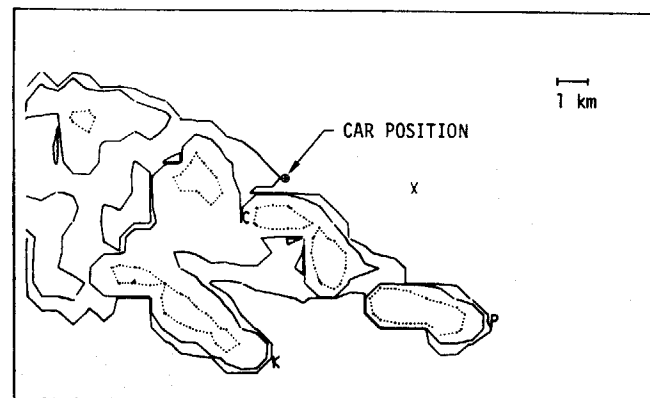


Lange - Fig. 11



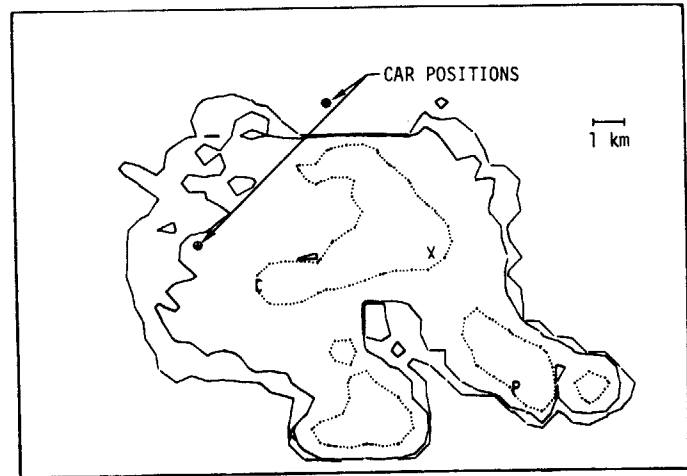
TOTAL x - y PLANES CYCLE258 TIME 13:00 EDT

Lange - Fig. 14



RELATIVE CONCENTRATION AT 2. METERS TIME IS 5.0 HOURS
 ISOPLETHS 5×10^{-7} 5×10^{-8} 5×10^{-9} s/m^3

Lange - Fig. 15



RELATIVE CONCENTRATION AT 2. METERS TIME IS 6.0 HOURS
ISOPLETHS 5×10^{-7} 5×10^{-8} 5×10^{-9} s/m^3

Lange - Fig. 13